



This is a repository copy of *Pulmonary MR angiography and perfusion imaging—A review of methods and applications*.

White Rose Research Online URL for this paper:
<http://eprints.whiterose.ac.uk/117014/>

Version: Accepted Version

Article:

Johns, C.S. orcid.org/0000-0003-3724-0430, Swift, A.J., Hughes, P.J.C. et al. (3 more authors) (2017) Pulmonary MR angiography and perfusion imaging—A review of methods and applications. *European Journal of Radiology*, 86. pp. 361-370. ISSN 0720-048X

<https://doi.org/10.1016/j.ejrad.2016.10.003>

Article available under the terms of the CC-BY-NC-ND licence
(<https://creativecommons.org/licenses/by-nc-nd/4.0/>).

Reuse

This article is distributed under the terms of the Creative Commons Attribution-NonCommercial-NoDerivs (CC BY-NC-ND) licence. This licence only allows you to download this work and share it with others as long as you credit the authors, but you can't change the article in any way or use it commercially. More information and the full terms of the licence here: <https://creativecommons.org/licenses/>

Takedown

If you consider content in White Rose Research Online to be in breach of UK law, please notify us by emailing eprints@whiterose.ac.uk including the URL of the record and the reason for the withdrawal request.



eprints@whiterose.ac.uk
<https://eprints.whiterose.ac.uk/>

PULMONARY MR ANGIOGRAPHY AND PERFUSION IMAGING – A REVIEW OF METHODS AND APPLICATIONS

AUTHORS: CHRISTOPHER S JOHNS¹, ANDREW J SWIFT¹, PAUL JC HUGHES¹, MARK SCHIEBLER², AND JIM M. WILD¹.

¹UNIVERSITY OF SHEFFIELD, UK

² UW-MADISON SCHOOL OF MEDICINE AND PUBLIC HEALTH, MADISON, WI, USA

Corresponding author: Jim Wild, j.m.wild@sheffield.ac.uk

INTRODUCTION

The role of the respiratory system is to ensure adequate exchange of oxygen and carbon dioxide for the body's metabolic requirements. This process of gas exchange requires adequate ventilation, passive diffusion across the alveolar surface and pulmonary perfusion. The assessment of pulmonary perfusion is therefore important in further understanding multiple physiological and pathophysiological mechanisms and also in the diagnosis and follow up of multiple pulmonary diseases.

There are two broad approaches in MR imaging of the pulmonary circulation. Higher spatial, but lower temporal resolution MR angiography (MRA) allows for assessment of the structure of the pulmonary arterial and venous system. Whilst lower spatial but higher temporal resolution perfusion MRI allows for the assessment of capillary level tissue perfusion (1).

Current clinical practice relies upon CTPA for the structural analysis of the pulmonary vasculature: it is readily available, fast, cheap and offers high spatial resolution. However, it requires exposure to approximately 5 mSv of ionising radiation, which is associated with increased risk of cancer and requires the use of iodinated contrast media, which is contraindicated in allergy or renal failure. Single photon emission computed tomography (SPECT) is currently the mainstay of clinical perfusion imaging. This requires injection of 100MBq of ^{99m}Tc labelled macro-aggregated human albumin, resulting in exposure to ionising radiation with an effective dose of 3mSv (2). Beyond exposure to ionising radiation the limitations of SPECT include: low spatial and temporal resolution, soft tissue attenuation (for example breast tissue or obesity) and movement from the diaphragm.

Historically, pulmonary MRI has been limited by poor signal due to: low proton density; susceptibility differences between multiple air-tissue interfaces causing short $T2^*$; and motion artefact from the heart and breathing (1,3,4). However, improvements in scanner hardware and short echo time pulse sequences combined with parallel imaging and view sharing techniques have allowed for reduced acquisition times, counteracting the short $T2^*$ and movement artefacts. Imaging of pulmonary perfusion and particularly its quantification is further complicated by a number of physiological processes. There are

physiological differences in pulmonary blood flow in expiration and inspiration (1). Furthermore there are anatomical differences in regional perfusion due to gravity, causing an apico-basal gradient when erect (5) or an antero-posterior gradient when supine (6). This perfusion heterogeneity is reduced in the prone position (7). Consideration is also required of the dual circulatory systems in the lungs: the pulmonary arteries carry deoxygenated blood from the right ventricle to the lungs to be oxygenated and the bronchial arteries carry oxygenated blood from the aorta to supply the pulmonary parenchyma with its metabolic requirements (1). Moreover, the pulmonary arteries and veins have a similar anatomical distribution and can be hard to distinguish so it is therefore important to ensure that the correct “phase” of blood flow is imaged. MRI of the lungs is also further constrained by patient factors: patients who are short of breath may not be able to breath-hold for much longer than 10 seconds and patient positioning and claustrophobia can also lead to scanning difficulties with movement artefacts or abortion of scans.

CONTRAST ENHANCED METHODS

CONTRAST ENHANCED MRA

T1 shortening contrast agents can be used to produce high spatial resolution images of the pulmonary arteries and veins with 3D acquisitions within a single breath-hold. Currently this method is the mainstay of pulmonary MRA in the clinical setting. Typically, a bolus of gadolinium-chelated agent is administered into a large vein, usually in the antecubital fossa followed by a saline flush. Typical contrast doses are 0.1 mmol/kg body weight Gadovist followed by a 20ml saline flush injected at 5ml/sec. In order to reduce venous contamination and gain greatest arterial and venous separation, a single dose of gadolinium at a high injection rate should be used.

The contrast administration is followed by acquisition of a T1 weighted 3D gradient echo dataset. Typical imaging parameters are: TR=2.5-3 ms, TE=1.0-1.5 ms, $\alpha=30-40^\circ$, matrix=40×192×256, FOV=460 mm, parallel imaging factor R=2 (3). In order to synchronise image acquisition with peak contrast enhancement in the pulmonary vessels, a bolus tracking technique can be employed: a test bolus with a time resolved

test scan is used to assess the optimal time from injection to acquisition of central k-space, resulting in images from a single time point (3). An important consideration in pulmonary MRA is the rapid transit of blood through the lungs (3-5 seconds). Centric elliptic phase encoding, with the scan acquisition starting at peak enhancement ensures maximum SNR and optimal separation of arterial and venous phases.

The contrast bolus passage may also be imaged with time resolved 3D view sharing acquisitions, such as TRICKS (Time Resolved Imaging of Contrast KineticS), allowing for haemodynamic assessment of the pulmonary circulation. These view-sharing methods under-sample k-space and share missing k-space between datasets, giving a higher nominal temporal resolution, with the risk of spatio-temporal interpolation artefacts. Other methods for k-space sampling such as spiral acquisition and view sharing can further reduce scan times, with some centres producing high spatial resolution MRA images with temporal resolution of 1 second through spiral-TRICKS acquisition (8).

Whilst the majority of clinical MRA is currently performed using extracellular contrast media such as gadobutrol (Gadovist TM) and gadobenate dimeglumine (Multihance TM), there is also the potential to perform pulmonary MRA using intravascular (blood pool) media such as Gadomer-17, Gadofosveset trisodium and ferumoxytol (9). The long residency time of these agents can enable high SNR and spatial resolution with averaging over several breath-holds, however arterial and venous phase separation is sacrificed (9). Blood pool agents for clinical pulmonary MRA is very helpful in patients that cannot hold their breath as non breath-hold heavily averaged MRA acquisition methods can be used.

DYNAMIC CONTRAST ENHANCED PERFUSION MRI

With a similar methodology to contrast enhanced MRA but using lower spatial and higher temporal resolution image acquisition, T1-weighted dynamic contrast enhanced (DCE) perfusion images of the first pass of a gadolinium contrast bolus can be performed. Typical imaging parameters would be: TR=2.0-2.5ms, TE=0.8- 1.0ms, $\alpha=30-40^\circ$, matrix=32×96×128, FOV=460mm. A lower dose of contrast is needed e.g. 0.05ml per kg patient weight of gadobutrol (Gadovist TM). Again, the nominal temporal resolution of the acquisition can be increased with parallel imaging and view sharing (1) but this can result in spatio-

temporal blurring of the signal. In clinical practice, images acquired with a frame rate of around 0.5 s per 3D lung volume can preserve spatial resolution sufficient for diagnostic purposes.

Perfusion images can be qualitatively assessed by subtraction of the baseline dataset from the peak enhancement dataset, allowing for a rapid assessment of perfusion defects and their anatomical location. With more detailed post-processing of the entire time resolved data, quantitative assessment of contrast passage kinetics can be made. Pulmonary blood flow (PBF), pulmonary blood volume (PBV) and mean transit time (MTT) can then be quantified and parametric maps of these metrics can be generated from voxel-wise analysis. For absolute quantitative analysis an arterial input function (AIF) is measured in a large feeding artery, often the main pulmonary artery for lung imaging (3).

Once the AIF has been established, the signal time curve of a voxel can be converted to concentration time course from the assumption of a linear relationship between signal intensity and contrast concentration. A model free approach using the following equation can be used:

$$C(t) = k \frac{S(t) - S_0}{S_0}$$

Where $S(t)$ is the signal time-course, S_0 is the mean signal before contrast enhancement and k is an unknown constant. For absolute quantitative analysis, T_1 mapping is required in order to convert signal intensity to contrast agent concentration (mmol/litre (mM)). One method of T_1 mapping used in quantitative perfusion analysis is the variable flip angle approach. Using a Levenberg-Marquardt fitting algorithm tissue density at equilibrium (m_0) and T_1 relaxation at equilibrium can be calculated via:

$$s(\alpha) = m_0 \sin \alpha \frac{1 - E1_0}{1 - \cos \alpha \cdot E1_0}$$

Where $E1_0 = \exp(-TR \cdot R1_0)$. TR = repetition time used in acquiring the T_1 -weighted flip angle images. Most commonly three values of flip angle (α) are used generally in the range of 2-35°. 4D post-injection longitudinal relaxation rates $R1(t)$ are then calculated:

$$R1(t) = -\left(\frac{1}{TR}\right) \cdot \ln \frac{1 - (A + B)}{1 - \cos \alpha \cdot (A + B)}$$

Where α = flip angle, $A = [S(t) - S(0)]/(M_0 \sin \alpha)$, $B = (1 - E1_0)/(1 - \cos \alpha E1_0)$. Gadolinium concentration maps can then be calculated using the equation:

$$C(t) = \frac{R1(t) - R1_0}{\mathfrak{R}1}$$

Where $\mathfrak{R}1$ is the experimental relaxivity of Gadolinium (4.39 s⁻¹ mM⁻¹ at 37 °C) (10). Following contrast concentration mapping the concentration time-curves are fitted using the Gamma variate function:

$$C(t) = K(t - AT)^a e^{- (t - AT)^b}$$

Where K is a constant scale factor, t is time after injection, AT is appearance time of the contrast agent in the voxel and a/b are arbitrary parameters. It is worthwhile noting that for gadolinium based contrast agents, unlike iodinated contrast agents, contrast concentration and signal intensity are not linearly related at higher concentrations. Constant K is related to tissue density, imaging sequence parameters, contrast agent and inspiration level. Hence, it is important that these are kept constant during the experiment (11). Following the indicator dilution theory (12), once the concentration time course of the AIF is known, $C_{AIF}(t)$, pulmonary blood flow (PBF) can be calculated:

$$C_{VOI}(t) = PBF \int_0^t C_{AIF}(\tau) \cdot R(t - \tau) d\tau = PBF [C_a(t) \otimes R(t)]$$

Where $C_{VOI}(t)$ is the contrast time course of the region of interest, R is the concentration of contrast remaining at time t and \otimes denotes the convolution integral (11,13). Pulmonary blood volume (PBV) and mean transit time (MTT) are defined as (13):

$$PBV = \frac{\int_0^\infty C_{VOI}(t) dt}{\int_0^\infty C_{AIF}(t) dt}$$

$$MTT = \frac{PBV}{PBF}$$

Noise filtering is required before these calculations can be reliably made (11) since the inherent image SNR is low. In order for perfusion quantification, it is assumed that there is a linear relationship between signal and concentration. This is not a true assumption and linearity is only seen in a small range of low concentrations of contrast. This is a particular problem for the AIF as the contrast passes in a compact

bolus (i.e. high concentration) (14). A robust contrast administration protocol is therefore paramount. One method for overcoming this is to use a smaller dose of contrast such as 0.05ml/kg at a rate of 4ml/second as suggested above. This has the advantage of only requiring a single injection, but with a reduction in SNR in the perfusion image. Another method is to use 2 boluses: a low dose injection to calculate the AIF and a second larger dose to give better SNR in the lung perfusion image (15). When using this split bolus technique the AIF must be recalculated to match the bolus used in the lung imaging part of the sequence. As contrast kinetics are involved, the bolus used to calculate the corrected AIF is shifted by injection duration τ (16):

$$C_{AIF}(t) = \sum^{V/V_p} C_p(t + q\tau)$$

It is also important to ensure that there is sufficient time between the first and second bolus to allow for wash-out of contrast.

NON-CONTRAST ENHANCED MRA AND PERFUSION IMAGING

Long acquisition times and problems with artefacts, such as motion, have limited the use of non-contrast enhanced MRA. Improving MR technologies, concerns about the use of gadolinium from the risk of nephrogenic systemic fibrosis (17) and the desire for non-invasive techniques for paediatrics have increased the motivation for non-contrast enhanced methodology for MR perfusion and angiography.

Double inversion recovery fast spin echo (DIR FSE) imaging, also known as black blood imaging, provides images of the pulmonary vasculature where the flowing blood returns no signal. This is particularly useful in the assessment of slow flow or thrombo-embolic disease, which are shown as an area of high signal intensity surrounded by the low signal intensity of flowing blood. The vessel walls are also well visualised.

ECG gated 3D partial-Fourier Fast Spin Echo (FSE) sequences utilise the difference between fast flow and slow flow on T2 signal. In systole, arterial flow is fast and causes a void of T2 signal, whereas in

diastole, flow is reduced and returns high T2 signal. Venous systems have slow flow in systole and diastole. Hence, a subtraction image of the systolic from diastolic image gives high T2 signal in the arterial system (18). This method requires ECG gating to allow separation of the diastolic and systolic images, and brings with it the risk of mis-registration.

Balanced steady-state free precession (bSSFP) produces images with the signal proportional to the $T2/T1$, through refocusing gradient echoes and alternating phases of RF pulses to create a coherent steady state. The TR must be kept very short as bSSFP is susceptible to field inhomogeneity (19). SSFP is particularly useful in imaging the blood, which has long T2 when compared to the surrounding tissues (3) and has short acquisition times allowing for short breath-holds (19). The high contrast between pulmonary blood pool and lumen make bSSFP an effective tool for assessment of thrombus when MRA and CTPA are inconclusive (20) and a fast 3D bSSFP acquisition provides a quick and contrast free means of generating a pulmonary angiogram (21).

Arterial spin labelling (ASL) images are produced by radiofrequency excitation of the water protons in blood upstream of the imaging field of view through an inversion pulse. These “tagged” protons then flow into the field of view to be imaged (14,18,22). A control image is also taken and the images tend to be presented as a subtraction of the control image from the tagged image. ASL in the lungs is challenging as ECG gating requires a regular heartbeat (14), but can be improved with newer labelling techniques including continuous arterial spin labelling (CASL), pulsed arterial spin labelling (PASL) and a combination as pseudo-continuous arterial spin labelling (pCASL) (23). ASL using the spin echo entrapped perfusion image (SEEPAGE) allows for a single shot acquisition within 5 seconds. SEEPAGE completely suppresses the background tissue, so only the “tagged” protons flowing into the field of view return signal. This has the advantage of requiring no subtraction (so no mis-registration) and allows rapid acquisitions within short breath-holds (24). All of these spin-labelling techniques are by nature slice selective methodologies, and therefore limited in terms of lung volume coverage.

Time of flight (TOF) MRA is commonly used in neurovascular and peripheral vascular imaging, but poor spatial resolution, sensitivity to motion (cardiac or respiratory), multiplanar flow directionality and insensitivity to slow flow and sensitivity to susceptibility artefacts limits the utility of TOF MRA in the lungs (25).

Phase contrast MRA with velocity sensitizing gradients can be used to quantitatively map the blood flow in the major vessels in the lungs in 3-dimensions and can provide insight in to pulmonary vascular resistance and non-steady and turbulent flow in the pulmonary arteries (1,18). Typical velocity encoding settings of v_{enc} 150cm/s would be used to map flow in the pulmonary artery but this may need adjustment for slower flow in diseases such as pulmonary hypertension where flow velocity is slower and directionality is helical. Recent developments with 3D view shared phase contrast methods allow 3D time resolved imaging of blood flow in the pulmonary arteries (26). Recent developments with 3D view shared phase contrast methods allow for the acquisition of 4D flow in the pulmonary arteries (26,27).

Time resolved imaging of the lungs during free breathing with Fourier decomposition (FD) analysis can be used as a surrogate method to image lung perfusion without the need for contrast or ECG gating. Fourier decomposition has recently been applied to lung ventilation and perfusion imaging (28). During inspiration the lungs increase in volume, reducing parenchymal signal, increasing again in expiration. During systole, high blood velocity causes dephasing of the MR signal, reducing signal. The respiratory changes occur at a rate of 12-20 beats per minute and the cardiac changes at a rate of 60-80 beats per minutes on average. The difference in frequencies allows for separation using Fourier Decomposition (FD), to give ventilation weighted or perfusion weighted images (29) which have been used for perfusion quantification (30).

CLINICAL APPLICATIONS OF PULMONARY MRA AND PERFUSION IMAGING

An area that has had significant interest for MR angiography and perfusion is in the assessment of pulmonary emboli (PE)(25), particularly in young or pregnant patients who benefit from the avoidance of

radiation exposure. Real time MR with SSFP (True FISP) produces T2 weighted images in which blood in the pulmonary arteries is bright and thrombus is dark. A major advantage of this method is that it is unaffected by patient movement. A study of 39 cases with suspected PE gave sensitivity of 83% and specificity of 100% for the diagnosis of acute PE (31). Further studies using contrast enhanced MRA have also shown sensitivity similar to that of SPECT and CTPA (32,33) . However, the PIOPED III study, conducted in seven centres, assessing 371 patients (104 with PE) using contrast enhanced MRA, was less optimistic. They found that 25% of patients had inadequate image quality, with the majority of these due to poor arterial opacification and motion artefacts. Sensitivity and specificity for acute PE were 78% and 99%, although this is increased when combined with venography (34). The lower spatial resolution of MRA over CTPA may account for this low sensitivity. The PIOPED researchers recommend that MRA for acute PE is only performed in certain centres who regularly perform it, and only in patients with contraindications to standard tests. The perfusion defects from obstruction of the pulmonary vascular bed have a characteristic wedge shape. DCE MRI has been shown to have a high agreement with SPECT (35). Quantitative assessment of perfusion can also predict the presence of acute PE and predict outcome, with PBF being the most accurate parameter (36). Interestingly, two sites (UW-Madison and U of Arizona) have been using contrast enhanced MRA for the primary diagnosis of pulmonary embolism in young women and in patients with iodinated contrast allergy with good results (32). The negative predictive value of MRA for the exclusion of pulmonary embolism is >97%. More recent data recently presented by the UW-Madison group has shown even better outcomes (NPV 99%) (37). There is a performance gap between the efficacy (sensitivity and specificity of MRA vs CTA for PE detection) of MRA from the PIOPED III study and the real world performance of this test (effectiveness). This may be related to the fact that sub segmental PE, which are not well seen on contrast enhanced MRA, are not clinically significant. These results will need to be repeated at other sites, but suggest that there has been premature abandonment of this imaging test for the primary diagnosis of PE. The use of MRA can also be performed as a follow-up for known pulmonary embolism to mitigate the amount of medical radiation for these patients.

Perfusion MRI may be particularly useful in the assessment of chronic PE. It has been shown that MR perfusion can be used to screen for perfusion defects in patients with chronic thrombo-embolic pulmonary hypertension (CTPEH) (38) and can differentiate the perfusion patterns of CTPEH and idiopathic pulmonary artery hypertension as they have focal defects or diffuse reduction in perfusion respectively (39). Further work has shown that contrast enhanced MRA and non-contrast enhanced MRA with SSFP can be used to diagnose CTPEH with a high sensitivity, with the SSFP imaging being particularly useful in identifying proximal disease, but is limited for sub segmental disease (20). PBF has been shown to improve in CTPEH patients who have had pulmonary endarterectomy (40). There is also an increase in MTT in patients with pulmonary arterial hypertension (PAH), which shows a modest correlation with mPAP (41,42) and in patients with combined emphysema and fibrosis MTT correlates with mean pulmonary artery pressure and pulmonary vascular resistance (43). In addition, in patients with PAH, pulmonary transit times have been shown to correlate with markers of disease severity, mean right atrial pressure and pulmonary vascular resistance (44) and are predictive of mortality at univariate analysis and have equivalent prognostic value to invasive measures taken at right heart catheterisation (45). Analysis of pulmonary arterial flow is also proving to be useful in pulmonary hypertension. Sanz et al showed that average pulmonary arterial velocity showed a strong correlation with mean pulmonary artery pressure (46) and 4D phase contrast MRI is also providing insights into the complex flow pattern that occur in pulmonary hypertension patients. Reiter et al. showed that patients with pulmonary hypertension have vortices in their pulmonary arterial blood flow, whereas healthy volunteers did not. Furthermore they showed a very strong correlation between the duration of vertical blood flow and mean pulmonary arterial pressure (47).

In COPD the mean pulmonary blood flow (PBF), mean transit time (MTT) and pulmonary blood volume (PBV) are heterogeneous and decreased (13), likely due to regional hypoxic vasoconstriction. The perfusion defects seen in COPD can be differentiated from vascular obstruction as they are not wedge shaped (35). One study of 45 patients with COPD showed a high correlation in the distribution of MR perfusion defects and parenchymal destruction on CT (48). Patients with emphysema also show a loss of the normal physiological increase in PBV that is associated with expiration (49). DCE perfusion scores have

been shown to correlate with markers of COPD severity: a reduction in PBF and PBV is associated with worsening CT emphysema score, airflow limitation and DLCO (50,51). Furthermore, exacerbations of COPD are associated with a prolonged MTT and TTP (52).

In 11 children with cystic fibrosis (CF), it was shown that MRI perfusion defects correlated well with parenchymal abnormalities (53). In younger patients the changes are more prominent on perfusion MRI than morphological changes on CT, raising the possibility of an early biomarker for disease progression (54). Perfusion MRI may be used to monitor response to therapy (54) and differentiate reversible from irreversible regions of disease (55). This is particularly useful in CF, as the patients are young and repeated exposure to radiation from CT should be reduced. As these patients are young, a technique such as ASL or Fourier Decomposition, which require no cannulation or contrast injection would be beneficial and have shown promising results in young patients. Although they do rely upon good patient compliance (due to requirement of breath holds), challenging in young children (56).

The high spatial resolution of pulmonary MRA allows for the direct assessment of pulmonary vascular anatomy. This can be utilised to assess for pulmonary vascular abnormalities such as anomalous pulmonary venous return, pulmonary artery atresia and pulmonary artery arterio-venous malformations (AVMs) (1,57). Time resolved MRA, such as TRICKs, allows for assessment of right to left shunting (58), complementary to pulmonary to systemic (Qp:Qs) shunt assessment using pulmonary and aortic phase contrast imaging.

To date there is very limited information published on the role of perfusion MRI in pulmonary fibrosis. Whilst not directly related to perfusion, DCE-MRI can differentiate inflammatory and fibrotic lesions: inflammatory predominant biopsies showed early enhancement and fibrotic predominant biopsy sites showed late enhancement in 26 cases of fibrotic lung disease (59). Furthermore, a comparison of 27 systemic sclerosis and 10 healthy patients showed that there was a reduction in PBV corrected for lung volume (60). As there is a high incidence of PH in fibrotic lung disease, qualitative and quantitative measures of pulmonary perfusion would be an interesting area for future research.

Conclusion

Improvements in MRI technology have triggered increasing interest in pulmonary MR perfusion and angiography. Whilst multiple methods of image acquisition are available, the mainstay of current clinical use is contrast enhanced MRA and DCE MRI. Modest concerns regarding the widespread use of gadolinium based contrast agents and the requirement for IV access have increased interest in non-contrast enhanced techniques, although these methods are currently confined to research. Pulmonary MRA and MRI perfusion are routinely used in the clinical assessment of patients with pulmonary hypertension (PH). There is great potential for the role of MRI to be expanded in the diagnosis and serial assessment of patients with pulmonary embolism, cystic fibrosis, COPD and in the assessment of patients with pulmonary vascular abnormalities (such as arteriovenous malformations and anomalous venous drainage). Further methodological developments of MRI sequences coupled with clinical implementation of some of the techniques described, will help to further current understandings of pulmonary and pulmonary vascular disease.

BIBLIOGRAPHY

1. Hopkins SR, Wielpütz MO, Kauczor H-U. Imaging lung perfusion. *J Appl Physiol* [Internet]. 2012;113(2):328–39. Available from: <http://jap.physiology.org/content/113/2/328>
2. Reinartz P, Wildberger JE, Schaefer W, Nowak B, Mahnken AH, Buell U. Tomographic imaging in the diagnosis of pulmonary embolism: a comparison between V/Q lung scintigraphy in SPECT technique and multislice spiral CT. *J Nucl Med*. 2004;45(9):1501–8.
3. Wild JM, Marshall H, Bock M, Schad LR, Jakob PM, Puderbach M, et al. MRI of the lung (1/3): Methods. *Insights Imaging*. 2012;3:345–53.
4. Hatabu H, Gaa J, Kim D, Li W, Prasad P V, Edelman RR. Pulmonary perfusion: qualitative assessment with dynamic contrast-enhanced MRI using ultra-short TE and inversion recovery turbo FLASH. *Magn Reson Med*. 1996;36(4):503–8.
5. Anthonisen NR, Hospital RV. Distribution of pulmonary perfusion in erect man. *J Appl Physiol*. 1966;21(3):760–6.
6. Cao JJ, Wang Y, Schapiro W, McLaughlin J, Cheng J, Passick M, et al. Effects of respiratory cycle and body position on quantitative pulmonary perfusion by MRI. *J Magn Reson Imaging*. 2011;34(1):225–30.
7. Henderson AC, Sa RC, Theilmann RJ, Buxton RB, Prisk GK, Hopkins SR. The gravitational distribution of ventilation-perfusion ratio is more uniform in prone than supine posture in the normal human lung. *J Appl Physiol* [Internet]. American Physiological Society; 2013 Aug 1 [cited 2016 Jun 27];115(3):313–24. Available from: <http://www.ncbi.nlm.nih.gov/pubmed/23620488>
8. Du J, Bydder M. High-resolution time-resolved contrast-enhanced MR abdominal and pulmonary angiography using a spiral-TRICKS sequence. *Magn Reson Med* [Internet]. 2007 Sep;58(3):631–5. Available from: <http://doi.wiley.com/10.1002/mrm.21298>
9. Abolmaali ND, Hietschold V, Appold S, Ebert W, Vogl TJ. Gadomer-17-enhanced 3D navigator-echo MR angiography of the pulmonary arteries in pigs. *Eur Radiol* [Internet]. 2002;12(3):692–7. Available from: http://eutils.ncbi.nlm.nih.gov/entrez/eutils/elink.fcgi?dbfrom=pubmed&id=11870489&retmode=ref&cmd=prlinks\nhttp://download.springer.com/static/pdf/344/art%3A10.1007%2Fs00330-001-1221-1.pdf?auth66=1397827960_c7b66f7163e500589013b9ab132d35ad&ext=.pdf
10. Li KL, Zhu XP, Waterton J, Jackson A. Improved 3D quantitative mapping of blood volume and endothelial permeability in brain tumors. *J Magn Reson Imaging* [Internet]. 2000;12(2):347–57. Available from: <papers2://publication/uuid/13D475CA-9A96-41B9-9571-1BF93C036DE7>
11. Risse F. MR Perfusion of the Lung [Internet]. Kauczor H-U, editor. *MRI of the Lung*. Berlin, Heidelberg: Springer Berlin Heidelberg; 2009. 25-34 p. (Medical Radiology). Available from: <http://link.springer.com/10.1007/978-3-540-34619-7>
12. Meier P, Zierler KL. On the theory of the indicator-dilution method for measurement of blood flow and volume. *J Appl Physiol* [Internet]. 1954 Jun [cited 2016 Jun 23];6(12):731–44. Available from: <http://www.ncbi.nlm.nih.gov/pubmed/13174454>
13. Ohno Y, Hatabu H, Murase K, Higashino T, Kawamitsu H, Watanabe H, et al. Quantitative assessment of regional pulmonary perfusion in the entire lung using three-dimensional ultrafast dynamic contrast-enhanced magnetic resonance imaging: Preliminary experience in 40 subjects. *J Magn Reson Imaging* [Internet]. 2004;20(3):353–65. Available from: <http://www.ncbi.nlm.nih.gov/pubmed/15332240>

14. Ley S, Ley-Zaporozhan J. Pulmonary perfusion imaging using MRI: clinical application. *Insights Imaging* [Internet]. 2012;3(1):61–71. Available from: <http://link.springer.com/10.1007/s13244-011-0140-1>
15. Risse F, Semmler W, Kauczor H-U, Fink C. Dual-bolus approach to quantitative measurement of pulmonary perfusion by contrast-enhanced MRI. *J Magn Reson Imaging*. 2006;24(6):1284–90.
16. Köstler H, Ritter C, Lipp M, Beer M, Hahn D, Sandstede J. Prebolus quantitative MR heart perfusion imaging. *Magn Reson Med* [Internet]. 2004 Aug [cited 2016 Jun 23];52(2):296–9. Available from: <http://www.ncbi.nlm.nih.gov/pubmed/15282811>
17. Agarwal R, Brunelli SM, Williams K, Mitchell MD, Feldman HI, Umscheid CA. Gadolinium-based contrast agents and nephrogenic systemic fibrosis: A systematic review and meta-analysis. *Nephrol Dial Transplant*. 2009;24(3):856–63.
18. Miyazaki M, Lee VS. Nonenhanced MR angiography. *Radiology* [Internet]. 2008;248(1):20–43. Available from: <http://eutils.ncbi.nlm.nih.gov/entrez/eutils/elink.fcgi?dbfrom=pubmed&id=18566168&retmode=ref&cmd=prlinks\papers3://publication/doi/10.1148/radiol.2481071497>
19. Bitar R, Leung G, Perng R, Tadros S, Moody AR, Sarrazin J, et al. MR Pulse Sequences: What Every Radiologist Wants to Know but Is Afraid to Ask. *RadioGraphics* [Internet]. 2006 Mar;26(2):513–37. Available from: <http://pubs.rsna.org/doi/abs/10.1148/rg.262055063>
20. Rajaram S, Swift AJ, Capener D, Telfer A, Davies C, Hill C, et al. Diagnostic accuracy of contrast-enhanced MR angiography and unenhanced proton MR imaging compared with CT pulmonary angiography in chronic thromboembolic pulmonary hypertension. *Eur Radiol* [Internet]. 2012;22(2):310–7. Available from: <http://link.springer.com/10.1007/s00330-011-2252-x>
21. Bieri O. Ultra-Fast Steady State Free Precession and Its Application to In Vivo 1H Morphological and Functional Lung Imaging at 1.5 Tesla. *Magn Reson Med*. 2013;70:657–63.
22. Martirosian P, Boss A, Schraml C, Schwenzler NF, Graf H, Claussen CD, et al. Magnetic resonance perfusion imaging without contrast media. *Eur J Nucl Med Mol Imaging*. 2010;37(SUPPL. 1):52–64.
23. Gao Y, Goodnough CL, Erokwu BO, Farr GW, Darrah R, Lu L, et al. Arterial Spin Labeling - Fast Imaging with Steady-State Free Precession (ASL-FISP): A Rapid and Quantitative Perfusion Technique for High Field MRI. *NMR Biomed*. 2014;27(8):996–1004.
24. Fischer A, Pracht ED, Arnold JFT, Kotas M, Flentje M, Jakob PM. Assessment of pulmonary perfusion in a single shot using SEEPAGE. *J Magn Reson Imaging* [Internet]. 2008 Jan;27(1):63–70. Available from: <http://doi.wiley.com/10.1002/jmri.21235>
25. Van Beek EJR, Wild JM, Fink C, Moody AR, Kauczor HU, Oudkerk M. MRI for the Diagnosis of Pulmonary Embolism. *J Magn Reson Imaging*. 2003;18(6):627–40.
26. Barker AJ, Roldán-Alzate A, Entezari P, Shah SJ, Chesler NC, Wieben O, et al. Four-dimensional flow assessment of pulmonary artery flow and wall shear stress in adult pulmonary arterial hypertension: Results from two institutions. *Magn Reson Med* [Internet]. 2015 May;73(5):1904–13. Available from: <http://doi.wiley.com/10.1002/mrm.25326>
27. Markl M, Frydrychowicz A, Kozerke S, Hope M, Wieben O. 4D flow MRI. *J Magn Reson Imaging*. 2012;36(5):1015–36.
28. Bauman G, Scholz A, Rivoire J, Terekhov M, Friedrich J, De Oliveira A, et al. Lung ventilation- and perfusion-weighted Fourier decomposition magnetic resonance imaging: In vivo validation with hyperpolarized 3He and dynamic contrast-enhanced MRI. *Magn Reson Med*. 2013;69(1):229–37.
29. Bauman G, Puderbach M, Deimling M, Jellus V, Chefd’hotel C, Dinkel J, et al. Non-contrast-enhanced

perfusion and ventilation assessment of the human lung by means of Fourier decomposition in proton MRI. *Magn Reson Med.* 2009;62(3):656–64.

30. Kjørstad Å, Corteville DMR, Fischer A, Henzler T, Schmid-Bindert G, Zöllner FG, et al. Quantitative lung perfusion evaluation using fourier decomposition perfusion MRI. *Magn Reson Med.* 2014;72(2):558–62.
31. Kluge A, Müller C, Hansel J, Gerriets T, Bachmann G. Real-time MR with TrueFISP for the detection of acute pulmonary embolism: Initial clinical experience. *Eur Radiol.* 2004;14(4):709–18.
32. Schiebler ML, Nagle SK, François CJ, Repplinger MD, Hamedani AG, Vigen KK, et al. Effectiveness of MR angiography for the primary diagnosis of acute pulmonary embolism: Clinical outcomes at 3 months and 1 year. *J Magn Reson Imaging [Internet].* 2013 Oct;38(4):914–25. Available from: <http://doi.wiley.com/10.1002/jmri.24057>
33. Ohno Y, Higashino T, Takenaka D. MR Angiography with Sensitivity Encoding (SENSE) for Suspected Pulmonary Embolism : Comparison with MDCT and Ventilation–Perfusion Scintigraphy. *AJR Am J Roentgenol.* 2004;183(July):91–8.
34. Stein PD, Chenevert TL, Fowler SE, Goodman LR, Gottschalk A, Hales C a, et al. Gadolinium-Enhanced Magnetic Resonance Angiography for Pulmonary Embolism: A Multicenter Prospective Study (PIOPED III). *Ann Intern Med.* 2010;152(7):434–43.
35. Amundsen T, Torheim G, Kvistad KA, Waage A, Bjermer L, Nordlid KK, et al. Perfusion abnormalities in pulmonary embolism studied with perfusion MRI and ventilation-perfusion scintigraphy: An intra-modality and inter-modality agreement study. *J Magn Reson Imaging.* 2002;15(4):386–94.
36. Ohno Y, Koyama H, Matsumoto K, Onishi Y, Nogami M, Takenaka D, et al. Dynamic MR perfusion imaging: Capability for quantitative assessment of disease extent and prediction of outcome for patients with acute pulmonary thromboembolism. *J Magn Reson Imaging.* 2010;31(5):1081–90.
37. Schiebler M, Francois C, Repplinger M et al. Effectiveness of Pulmonary Contrast Enhanced Magnetic Resonance Angiography for the primary workup of pulmonary embolism. In: International Society for Magnetic Resonance in Medicine, Book of Meeting Abstracts 2016 (Singapore Annual Meeting and Exhibition, May 7-13, 2016):Oral abstract presentation number 1074, Friday 1009:1012 am.
38. Rajaram S, Swift AJ, Telfer A, Hurdman J, Marshall H, Lorenz E, et al. 3D contrast-enhanced lung perfusion MRI is an effective screening tool for chronic thromboembolic pulmonary hypertension: results from the ASPIRE Registry. *Thorax [Internet].* 2013;68(7):677–8. Available from: <http://www.ncbi.nlm.nih.gov/pubmed/23349220>
39. Ley S, Fink C, Zaporozhan J, Borst MM, Meyer FJ, Puderbach M, et al. Value of high spatial and high temporal resolution magnetic resonance angiography for differentiation between idiopathic and thromboembolic pulmonary hypertension: Initial results. *Eur Radiol.* 2005;15(11):2256–63.
40. Schoenfeld C, Hinrichs J, Renne J, Olsson KM, Gutberlet M, Welte T. MR Imaging – derived Regional Pulmonary Parenchymal Perfusion and Cardiac Function for Monitoring Patients with Pulmonary Hypertension before and after Pulmonary. *Radiology [Internet].* 2016;0(0):1–10. Available from: <http://pubs.rsna.org/doi/abs/10.1148/radiol.2015150765>
41. Ley S, Mereles D, Risse F, Grünig E, Ley-Zaporozhan J, Tecer Z, et al. Quantitative 3D pulmonary MR-perfusion in patients with pulmonary arterial hypertension: Correlation with invasive pressure measurements. *Eur J Radiol.* 2007;61(2):251–5.
42. Ohno Y, Hatabu H, Murase K, Higashino T, Nogami M, Yoshikawa T, et al. Primary pulmonary hypertension: 3D dynamic perfusion MRI for quantitative analysis of regional pulmonary perfusion. *AJR Am J Roentgenol [Internet].* 2007;188(1):48–56. Available from:

<http://eutils.ncbi.nlm.nih.gov/entrez/eutils/elink.fcgi?dbfrom=pubmed&id=17179345&retmode=ref&cmd=prlinks\papers3://publication/doi/10.2214/AJR.05.0135>

43. Sergiacomi G, Bolacchi F, Cadioli M, Angeli ML, Fucci F, Crusco S, et al. Combined pulmonary fibrosis and emphysema: 3D time-resolved MR angiographic evaluation of pulmonary arterial mean transit time and time to peak enhancement. *Radiology* [Internet]. 2010;254(2):601–8. Available from: <http://www.ncbi.nlm.nih.gov/pubmed/20093531>
44. Skrok J, Shehata ML, Mathai S, Girgis RE, Zaiman A, Mudd JO, et al. Pulmonary arterial hypertension: MR imaging-derived first-pass bolus kinetic parameters are biomarkers for pulmonary hemodynamics, cardiac function, and ventricular remodeling. *Radiology* [Internet]. 2012 Jun;263(3):678–87. Available from: <http://eutils.ncbi.nlm.nih.gov/entrez/eutils/elink.fcgi?dbfrom=pubmed&id=22509050&retmode=ref&cmd=prlinks\papers3://publication/doi/10.1148/radiol.12111001>
45. Swift AJ, Telfer A, Rajaram S, Condliffe R, Marshall H, Capener D, et al. Dynamic contrast-enhanced magnetic resonance imaging in patients with pulmonary arterial hypertension. *Pulm Circ* [Internet]. 2014 Mar [cited 2015 Oct 1];4(1):61–70. Available from: <http://www.pubmedcentral.nih.gov/articlerender.fcgi?artid=4070759&tool=pmcentrez&rendertype=abstract>
46. Sanz J, Kuschnir P, Rius T, Salguero R, Sulica R, Einstein AJ, et al. Pulmonary Arterial Hypertension: Noninvasive Detection with Phase-Contrast MR Imaging. *Radiology*. 2007;243(1):70–9.
47. Reiter G, Reiter U, Kovacs G, Olschewski H, Fuchsjäger M. Blood flow vortices along the main pulmonary artery measured with MR imaging for diagnosis of pulmonary hypertension. *Radiology* [Internet]. 2015;275(1):71–9. Available from: <http://www.ncbi.nlm.nih.gov/pubmed/25372980>
48. Ley-Zaporozhan J, Ley S, Eberhardt R, Weinheimer O, Fink C, Puderbach M, et al. Assessment of the relationship between lung parenchymal destruction and impaired pulmonary perfusion on a lobar level in patients with emphysema. *Eur J Radiol*. 2007;63(1):76–83.
49. Ley-Zaporozhan J, Ley S, Kauczor H-U. Morphological and functional imaging in COPD with CT and MRI: present and future. *Eur Radiol* [Internet]. 2008;18(3):510–21. Available from: <http://www.ncbi.nlm.nih.gov/pubmed/17899100>
50. Jang YM, Oh Y-M, Seo JB, Kim N, Chae EJ, Lee YK, et al. Quantitatively assessed dynamic contrast-enhanced magnetic resonance imaging in patients with chronic obstructive pulmonary disease: correlation of perfusion parameters with pulmonary function test and quantitative computed tomography. *Invest Radiol* [Internet]. 2008 Jun [cited 2015 Dec 14];43(6):403–10. Available from: <http://www.ncbi.nlm.nih.gov/pubmed/18496045>
51. Hueper K, Parikh M, Prince MR, Schoenfeld C, Liu C, Bluemke DA, et al. Quantitative and Semi-quantitative Measures of Regional Pulmonary Parenchymal Perfusion by Magnetic Resonance Imaging and their Relationships to Global Lung Perfusion and Lung Diffusing Capacity – The MESA COPD Study. 2010;48(Suppl 2):1–6.
52. Sergiacomi G, Taglieri A, Chiaravalloti A, Calabria E, Arduini S, Tosti D, et al. Acute COPD exacerbation: 3 T MRI evaluation of pulmonary regional perfusion – Preliminary experience. *Respir Med* [Internet]. Elsevier Ltd; 2014;108(6):875–82. Available from: <http://linkinghub.elsevier.com/retrieve/pii/S0954611114001279>
53. Eichinger M, Puderbach M, Fink C, Gahr J, Ley S, Plathow C, et al. Contrast-enhanced 3D MRI of lung perfusion in children with cystic fibrosis--initial results. *Eur Radiol*. 2006;16(10):2147–52.
54. Wielpütz MO, Puderbach M, Kopp-Schneider A, Stahl M, Fritzsche E, Sommerburg O, et al. Magnetic resonance imaging detects changes in structure and perfusion, and response to therapy in early cystic fibrosis lung disease. *Am J Respir Crit Care Med* [Internet]. 2014;189(8):956–65. Available

from: <http://www.ncbi.nlm.nih.gov/pubmed/24564281>

55. Biederer J, Mirsadraee S, Beer M, Molinari F, Hintze C, Bauman G, et al. MRI of the lung (3/3)—current applications and future perspectives. *Insights Imaging* [Internet]. 2012;3(4):373–86. Available from: <http://link.springer.com/10.1007/s13244-011-0142-z>
56. Schraml C, Schwenzer NF, Martirosian P, Boss A, Schick F, Schäfer S, et al. Non-invasive pulmonary perfusion assessment in young patients with cystic fibrosis using an arterial spin labeling MR technique at 1.5 T. *Magn Reson Mater Physics, Biol Med*. 2012;25(2):155–62.
57. Maki DD, Siegelman ES, Roberts DA, Baum RA, Gefter WB. Thoracic Imaging Malformations : Three-dimensional Gadolinium- enhanced MR Angiography — Initial Experience. 2001;(2):243–6.
58. Mohrs OK, Voigtlander T, Heussel CP, Bardeleben S, Duber C, Kreitner KF. [Morphologic and functional assessment of vascular abnormalities of the pulmonary vasculature by breath-hold MR techniques]. *Rofo* [Internet]. © Georg Thieme Verlag Stuttgart · New York; 2002 Apr [cited 2016 Jun 27];174(4):467–73. Available from: <http://www.thieme-connect.de/DOI/DOI?10.1055/s-2002-25115>
59. Yi CA, Lee KS, Han J, Man PC, Myung JC, Kyung MS. 3-T MRI for differentiating inflammation- and fibrosis-predominant lesions of usual and nonspecific interstitial pneumonia: Comparison study with pathologic correlation. *Am J Roentgenol*. 2008;190(4):878–85.
60. Kanski M, Arheden H, Wuttge DM, Bozovic G, Hesselstrand R, Ugander M. Pulmonary blood volume indexed to lung volume is reduced in newly diagnosed systemic sclerosis compared to normals--a prospective clinical cardiovascular magnetic resonance study addressing pulmonary vascular changes. *J Cardiovasc Magn Reson* [Internet]. 2013;15:86. Available from: <http://www.pubmedcentral.nih.gov/articlerender.fcgi?artid=3850930&tool=pmcentrez&rendertype=abstract>
61. Heye T, Sommer G, Miedinger D, Bremerich J, Bieri O. Ultrafast 3D balanced steady-state free precession MRI of the lung: Assessment of anatomic details in comparison to low-dose CT. *J Magn Reson Imaging* [Internet]. 2015 Sep;42(3):602–9. Available from: <http://doi.wiley.com/10.1002/jmri.24836>

Figure 1: A diagrammatic representation of the basic principles of MR angiography against perfusion MR

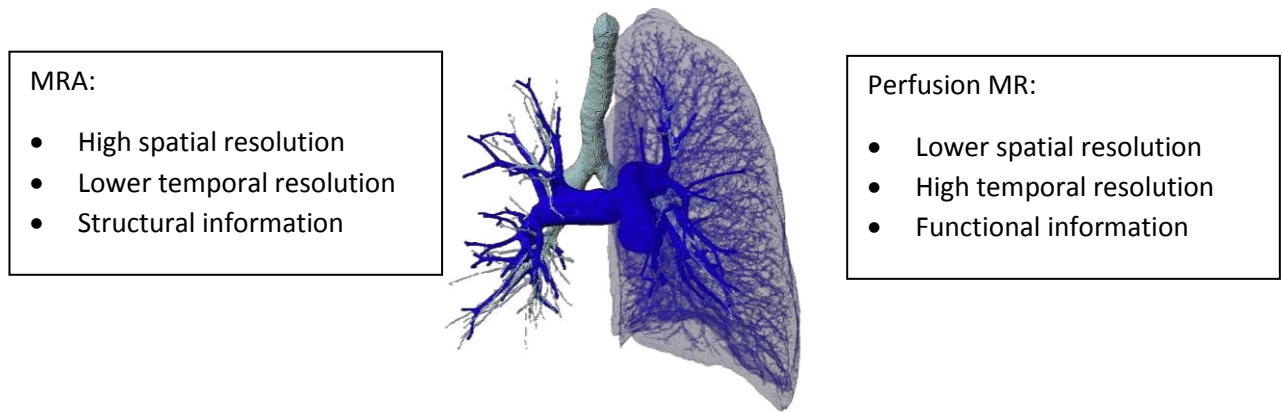
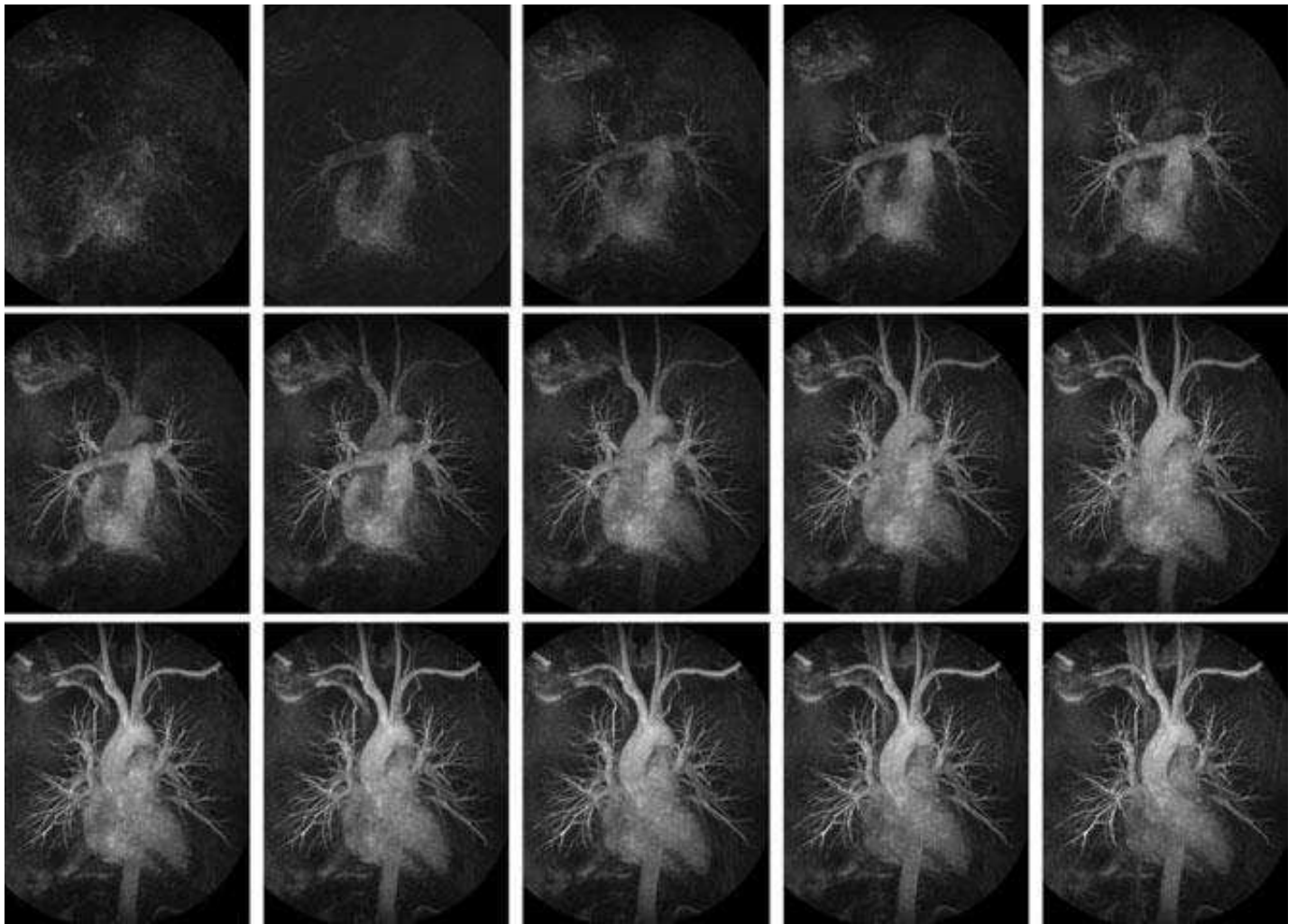


Figure 2:



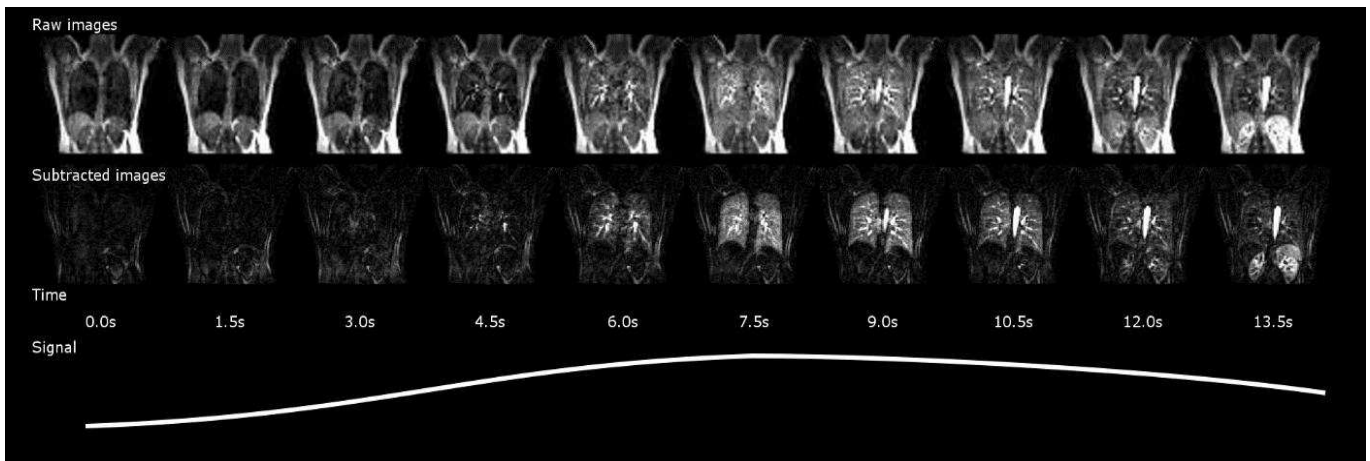
Legend Figure 2: A maximum intensity projection image from a normal contrast enhanced MR angiogram in a healthy volunteer. There is extensive venous contamination on this image, highlighting the importance of adequately timing the contrast bolus.

Figure 3.



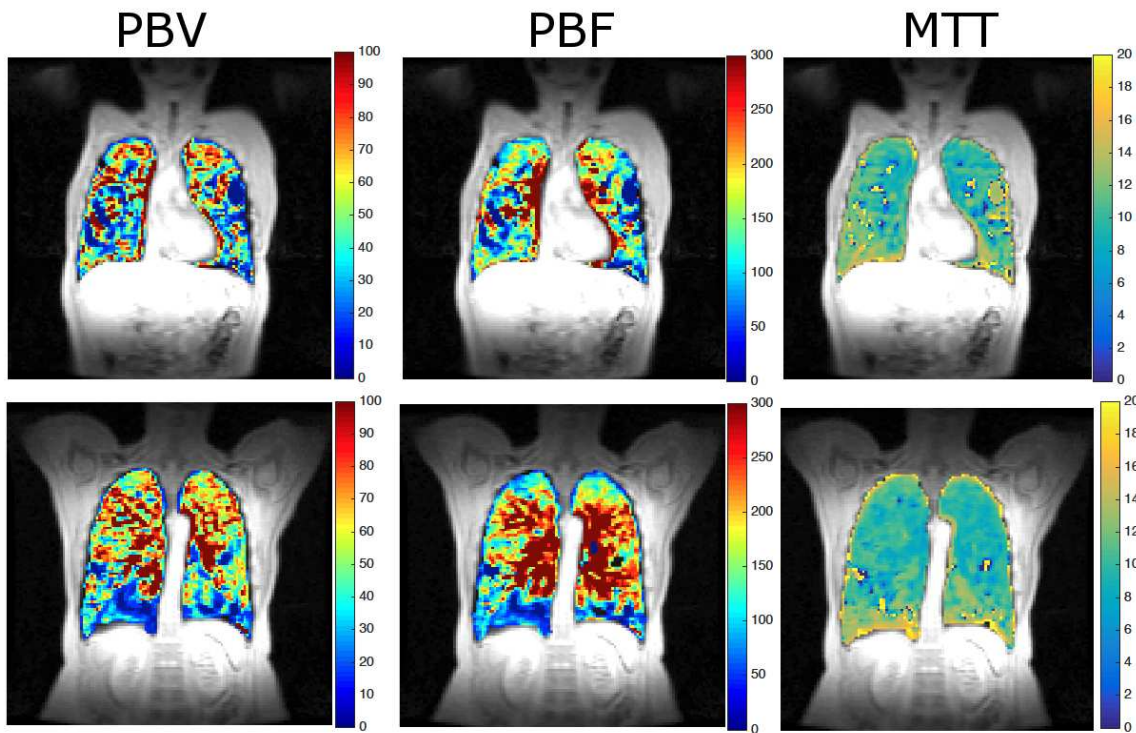
Legend figure 4: A normal MR angiogram showing contrast passage dynamics with 15 consecutive maximum intensity projection images with a temporal resolution of 1.0 sec/frame acquired using a spiral TRICKS technique. Image reprinted with permission from Wiley (8). © 2009 Wiley-Liss, Inc.

Figure 4:



Legend Figure 4: The time-course of dynamic contrast enhanced MRI showing a single coronal slice in a healthy volunteer. The top row of images shows the non-subtracted “raw” images, the second row shows the subtracted images and the bottom row shows the pulmonary parenchymal signal change over time. Please note that the images were acquired with a temporal resolution of 0.5 seconds but are displayed with a temporal resolution of 1.5 seconds.

Figure 5:



Legend Figure 5: Parametric maps of perfusion with a display of the Pulmonary Blood Volume (PBV), Pulmonary Blood flow (PBF) and Mean transit time (MTT) derived from post processing of a post contrast MR perfusion examination using the arterial input function in a patient with COPD. Please note the perfusion heterogeneity on the parametric maps.

Figure 6:

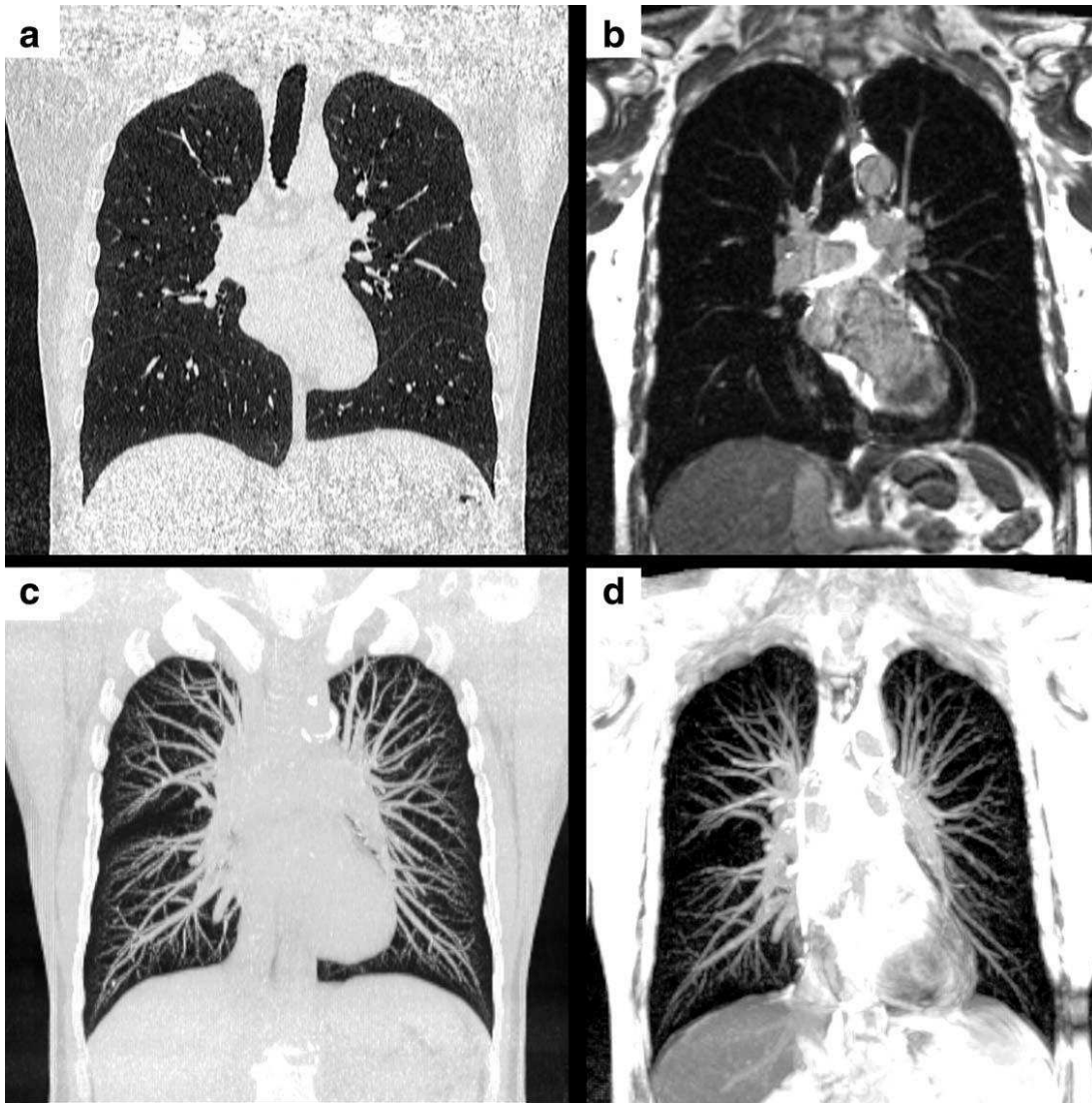
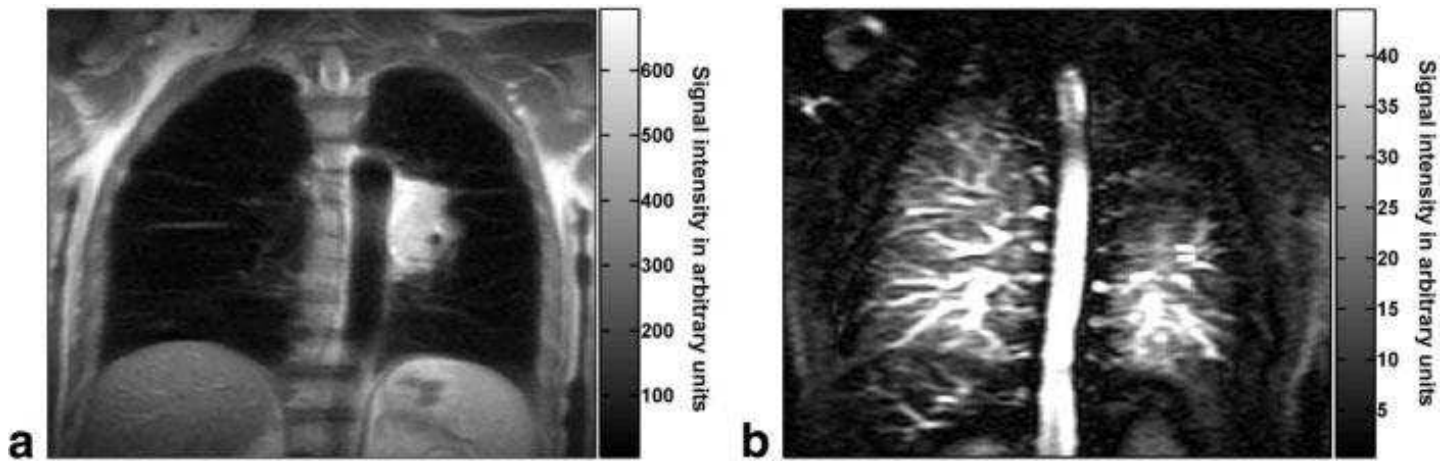


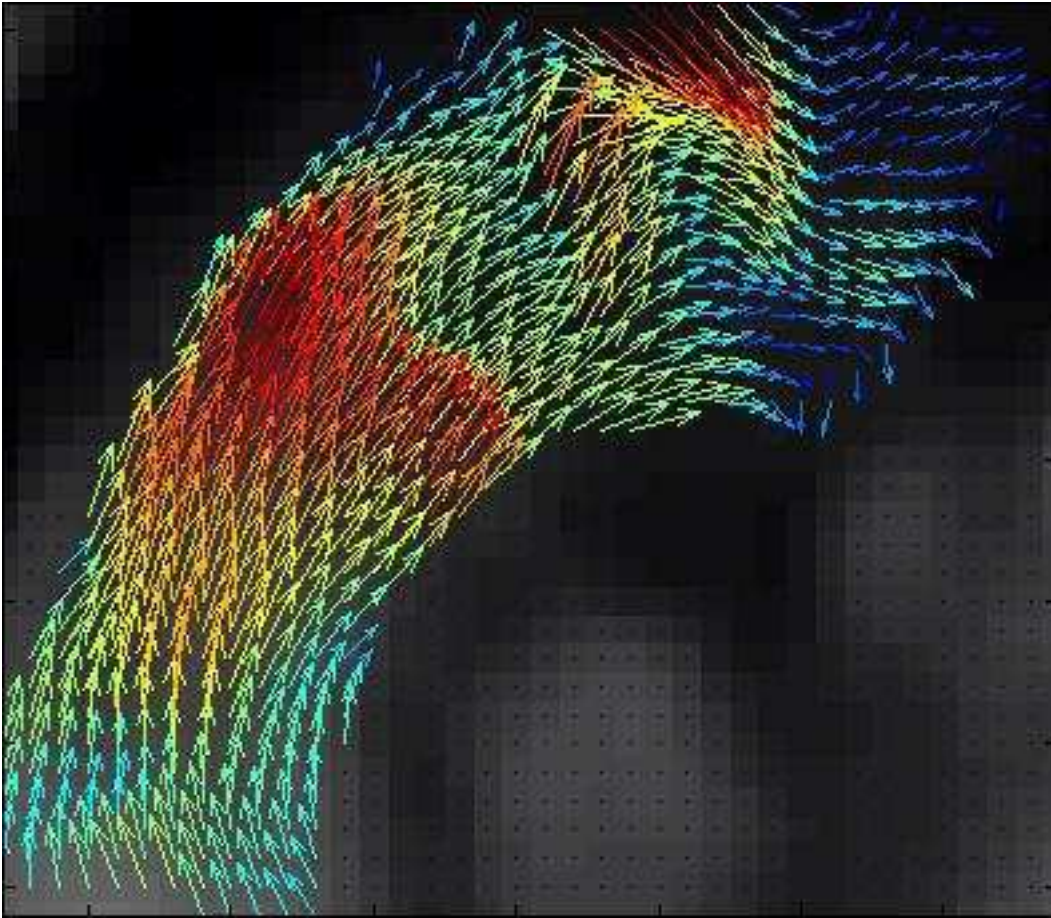
Figure 6 SSFP MRA: Comparison of 2mm slice coronal reconstructed unenhanced CT (a) with a 1.9mm isotropic bSSFP MR image (b) and 50mm maximum intensity image projections of the CT (c) and bSSFP MRI (d). Reproduced with permission from Wiley (61). © 2009 Wiley-Liss, Inc.

Figure 7:



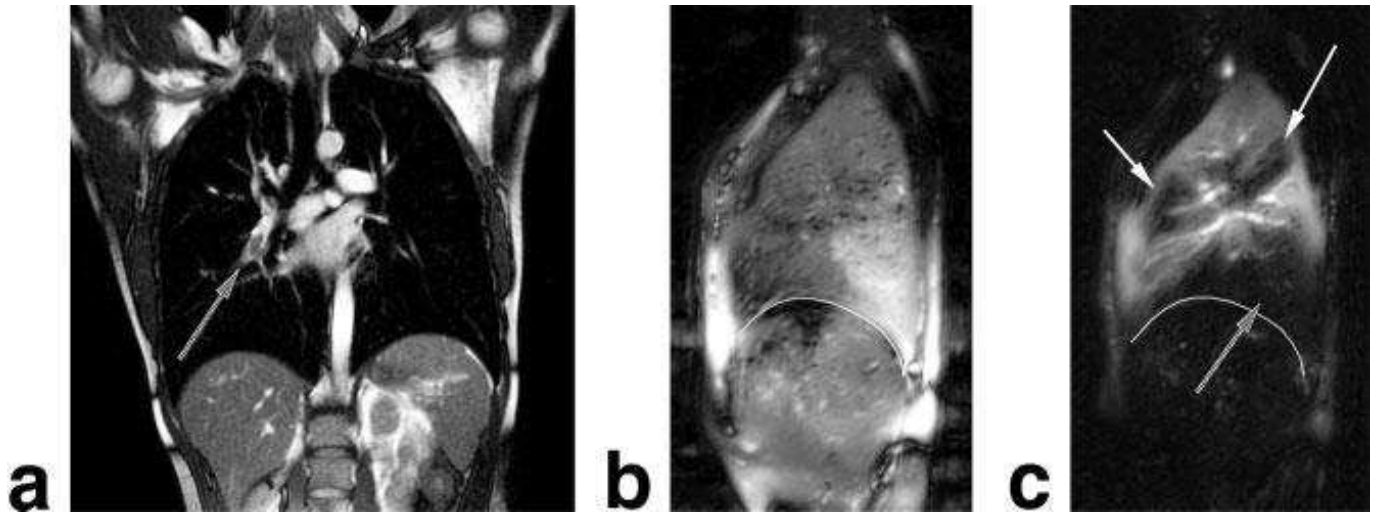
Legend Figure 7: Coronal HASTE image in a patient with a left hilar non-small cell lung cancer (a). A coronal perfusion weighted SEEPAGE image from more dorsal position (b), shows a large associated perfusion defect in the left upper lobe. This may be useful in planning for surgery and radiotherapy. Image reprinted with permission from Wiley (24). © 2009 Wiley-Liss, Inc.

Figure 8



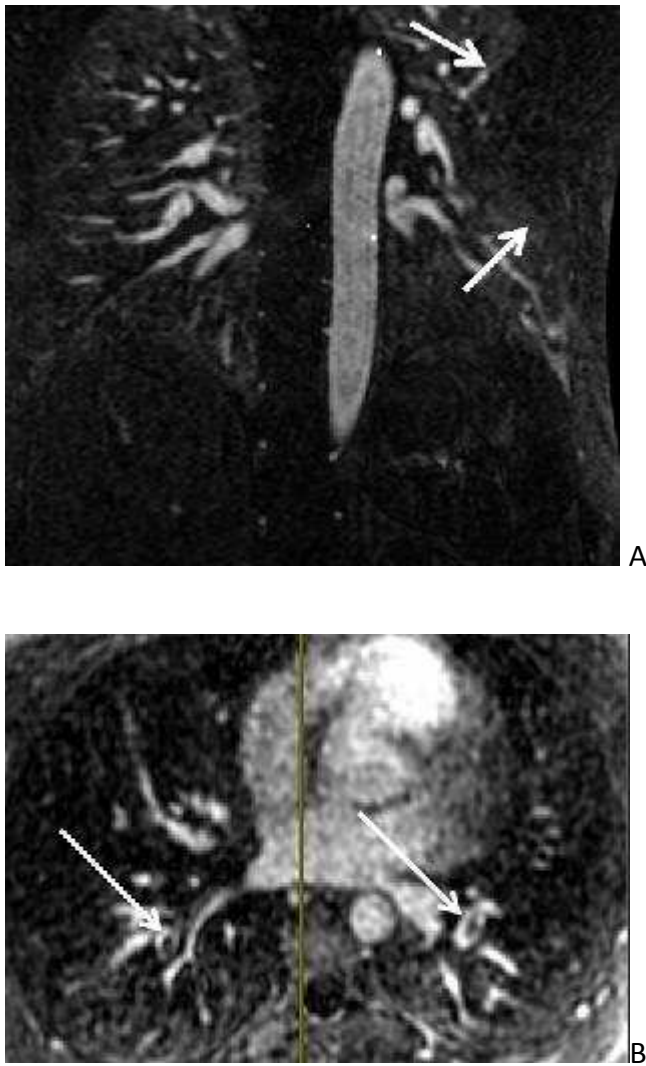
Legend Figure 8: 4D flow mapping vortices of blood flow in the pulmonary trunk showing mean voxel velocity and directionality of flow (Image courtesy of Dr Guilhem Collier, University of Sheffield).

Figure 9:



Legend figure 9: Image A shows a coronal TrueFISP image in a patient with right interlobar artery pulmonary embolus (arrow). The sagittal perfusion weighted Fourier Decomposition (c) image shows perfusion defects in the right upper and lower lobe, with no defect present on the corresponding ventilation/density image (b). These images (b and c) are examples of a ventilation perfusion mismatch using the Fourier decomposition method. Images reprinted with permission from Wiley (29). © 2009 Wiley-Liss, Inc.

Figure 10



Legend Figure 10: Twenty year old female college student presenting with a positive D-dimer to the student health service. 3D Contrast enhanced MRA in the coronal projection (A) was performed showing a left lower lobe perfusion defect (arrows) and the axial reformations show (B) bilateral pulmonary emboli (arrows). The patient was sent home on subcutaneous heparin and was advised to stop her oral contraception.